Rapid and low SAR B1-Mapping using a BURST-based Bloch-Siegert-Shift Sequence

Alexander Gotschy[1,2], Uvo C. Hölscher[3], Thomas C. Basse-Lüsebrink[1,4], André Fischer[5], Morwan Choli[3], Thomas Kampf[1], Volker Sturm[1], Daniel Neumann[3], Volker Herold[1], Herbert Köstler[5], Dietbert Hahn[5], Guido Stoll[4], Wolfgang R. Bauer[2], and Peter M. Jakob[1,3]

[1]Department of Experimental Physics 5, University of Würzburg, Würzburg, Germany, [2]Department of Internal Medicine I, University of Würzburg, Würzburg, Germany, [3]Research Center Magnetic Resonance Bavaria (MRB), Würzburg, Germany, [4]Department of Neurology, University of Würzburg, Würzburg, Germany, [5]Institute of Radiology, University of Würzburg, Würzburg, Germany

Introduction

For many MR applications an accurate knowledge of the B_1^+ field distribution becomes increasingly important. The knowledge of the B_1^+ field allows the detection of possible hotspots at ultrahigh fields and thus is essential for guaranteeing patient safety. Furthermore, it can deliver valuable information for B_1^+ shimming or Spatially Selective Excitation (SSE) algorithms. In 2010 Sacolick et al. introduced a Bloch-Siegert-Shift (BS) based B_1^+ mapping method which has already been applied to gradient echo (GE), standard spin echo and turbo-spin-echo (TSE) sequences [1,2]. To meet the requirements of high field imaging we extended the BS-methods to a BURST [3] sequence to combine robustness against T_2^* effects with reduced SAR. In the present study we compared linear against centric phase encoding which may provide additional robustness against T_2 effects. Thereby we found that the centric encoded BS-BURST sequences enable highly accelerated B_1^+ mapping with superior quality.

Methods

Measurements were performed on a conventional 3T clinical scanner and an experimental 7T human scanner. Fig. 1a displays the used BS-BURST sequence. After multiple low angle excitation pulses, two off-resonance pulses, one before (BS_1) and one after (BS_2) the refocusing pulse were applied to encode the B_1^+ information into the signal phase. The BS pulses were gaussian shaped with 5.12 ms duration and an off-resonance frequency of $\pm\omega_{off} = \pm 5$ kHz. For further information about B_1^+ field calculation, please refer to Sacolick et al. [1]. The number of applied excitation pulses has been termed BURST-Factor (BF) in the following. To optimize SNR, particularly at high BFs, we applied a phase cycling algorithm so that the excitation flip angle could be adjusted to $\alpha = 90°/\sqrt{BF}$. Fig. 1b shows the centric encoding schema for BF = 4 and a simplified matrix with 16 phase encoding steps. For 3T *in vivo* experiments the sequence parameters were: TR = 6 s, TE = 19 ms, FOV = 300x300 mm², MTX = 64x64, slices = 30. We evaluated SNR and the mean of the voxel wise standard deviation of the B_1 value (δB_1) in five independent measurements for BF = 4, 8, 16, 32 with linear and centric phase encoding in *in vivo* and phantom measurements. For *in vivo* measurements a head scan of a healthy volunteer was performed in accordance with institutional guidelines and after informed consent. For phantom measurements a T_1 doped water phantom was used. At 7T we artificially amplified a hotspot in a pineapple by fivefold increasing the RF power above the level of the regular adjustments, to test the sequence´s performance at very high and very inhomogeneous B_1^+ fields.

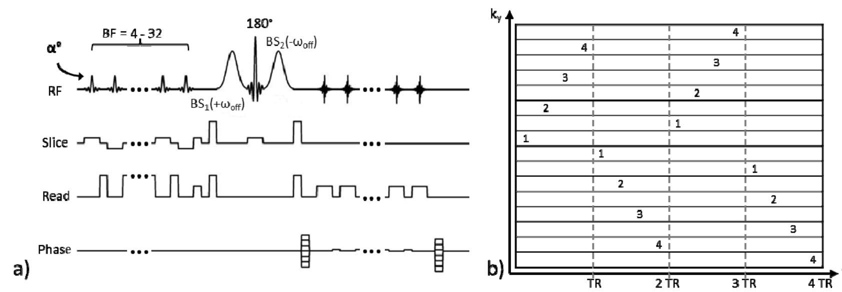

Fig. 1: a) Sequence diagram of the BS-BURST sequence. Slice selective excitation with interleaved acquisition was used to obtain information of 30 slices in one TR. **b)** Centric phase encoding schema with BF = 4 displayed for a simplified matrix with 16 phase encoding steps.

Results

Fig. 2b displays the flip angle map of the brain, obtained by a double angle experiment consisting of two GE experiments with a flip angle of 45° and 90°. The B_1^+ map calculated from the centric encoded BS-BURST experiments (Fig. 2c, BF= 32, slices = 30, TA= 36 s) shows good agreement with the flip angle map. In contrast the B_1^+ map calculated from the linear encoded BS-BURST experiments (Fig. 2d) shows a noisier B_1^+ distribution. The SNR for both encodings (Fig. 3a) was similar at small BF but using BF= 32 the centric encoding significantly outperformed linear encoding. In phantom measurements δB_1 showed hardly any difference between both encoding schemas (Fig. 3b). *In vivo*, however, the linear encoded BS-BURST showed a significant increase of δB_1 with higher BF whereas the centric encoded BS-BURST stayed constant only slightly above the level of the phantom scans. At 7T the BS-BURST sequence (BF= 4) showed extinction artifacts in the magnitude picture, however, a B_1^+ map could still be determined (Fig. 2e & 2f).

Conclusion

BS-BURST sequences allow the determination of B_1^+ maps at high field strength with lower SAR than other SE-based BS-sequences and are less sensitive to T_2* effects than GE-based BS-techniques. Thereby, centric encoding outperforms linear encoding regarding the B_1^+ map quality at high BFs. With BF=32 the B_1^+ information of a whole head was assessed in 36 s at 3T which makes the proposed technique suitable for applications in clinical routine. Compared to non BS-based ultrafast B_1^+ mapping techniques, like the Saturated Double Angle method, BS-BURST achieves higher stability against field inhomogeneity and T_1 effects at similar measurement times.

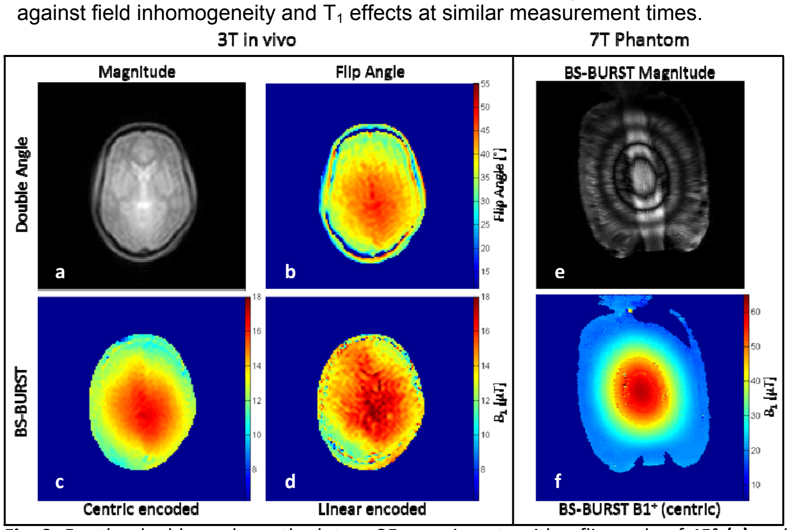

Fig. 2: For the double angle method, two GE experiments with a flip angle of 45° **(a)** and 90° were performed to obtain a flip angle map **(b)** of the brain. The BS-BURST experiments (BF = 32, slices = 30, TA = 36 s) with centric encoding **(c)** and linear encoding **(d)** were compared. At 7T the BS-BURST sequence (BF = 4, MTX = 256x256) shows extinction artifacts in the magnitude picture **(e)** but a B_1^+ map **(f)** could still be determined.

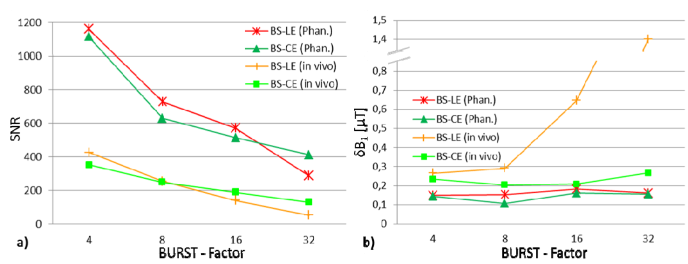

Fig. 3: SNR **(a)** and δB_1 **(b)** for BF = 4, 8, 16 and 32 with linear vs. centric encoding are compared for in vivo and phantom measurements.

References

[1] Sacolick L et al., Magn Reson Med (2010); 63:1315-1322
[2] Basse-Lüsebrink TC et al., Magn Reson Med (2011), DOI 10.1002/mrm.23013
[3] Henning J et al., MAGMA (1993) 1, 39--48

Acknowledgement

This work was supported by the DFG SFB 630, SFB 688 and the IZKF Würzburg project F-25. 7T measurements were performed at the DKFZ Heidelberg, Germany.